RSC Advances

PAPER

View Article Online
View Journal | View Issue

Cite this: *RSC Adv.*, 2019, **9**, 29255

Preparation and characterization of a nanolignin phenol formaldehyde resin by replacing phenol partially with lignin nanoparticles

Yu Chen, Xiaowu Gong, Gaoshan Yang, Qin Li and Na Zhou *

A new strategy for the preparation of a lignin phenol formaldehyde (LPF) resin has been developed. Nanolignin with high specific surface area and porous structure with an average particle size of about 300 nm was prepared, used as the raw material to substitute phenol partially, and combined with formaldehyde to produce a wood adhesive. The results show that the artificial board prepared with a nanolignin phenol formaldehyde (NLPF) resin with nanolignin substitution degree of 40% wt for phenol could give a dry bond strength of 1.30 ± 0.08 MPa, which is 1.85 times that of the Chinese national grade 1 plywood standard (0.7 MPa) and whose formaldehyde emission of 0.40 mg L^{-1} meets the standard of GB/T 14732-2006 (E_0, 0.5 mg L^{-1}). TG and DSC analyses show that the replacement of phenol by nanolignin could improve the thermal stability and decrease the curing temperature of the prepared lignin-based resin, with the residual ratio of 40% NLPF being 45% wt at 800 °C and the curing exothermic peak being 145.4 °C, which are much better than that of the 40% LPF resin with the residual ratio being 40% wt and the exothermic peak being 186 °C, respectively. The present study provides a new thought for preparation of LPF resins.

Received 26th June 2019
Accepted 1st September 2019

DOI: 10.1039/c9ra04827h

rsc.li/rsc-advances

1. Introduction

Adhesives have been playing a significant role in the wood manufacturing industry for the past several decades. Phenol formaldehyde (PF) resin, epoxy resin, and unsaturated polyester resin are considered to be the three main thermosetting resin adhesives.[1] The PF resin is a kind of synthetic polymer obtained from the reaction between phenol and formaldehyde.[2] Since the PF resin has the characteristics of low initial viscosity, strong water-resistance, and excellent thermal stability,[3,4] it has been widely used in the manufacture of plywoods, laminates, oriented strand boards, *etc.*[5] However, the raw materials used in the preparation of the PF resin, *viz.*, phenol and formaldehyde, are refined from petroleum products,[6,7] which are not only expensive but also non-renewable. At the same time, during the manufacture and application of the artificial board, the PF resin releases free aldehyde, which is a potential 2A-level carcinogen that can irritate the eyes, inflame the throat, and damage the respiratory tract.[8–10] In view of the increasing concerns towards human health and shortage of petroleum resources, the development of green and low toxicity wood adhesives has attracted much interest in the recent years.[11–14]

As a natural and non-toxic material,[15] lignin is an aromatic hydrocarbon polymer composed of phenylpropane units, with a large number of unsubstituted active hydrogen and phenolic hydroxyl groups in its benzene ring structure and numerous alcoholic hydroxyl and other active functional groups in its side chain, which make lignin a potential substitute for phenol in the synthesis and preparation of a lignin phenol formaldehyde (LPF) resin.[16–18] Some researchers replaced phenol partially with lignin to prepare the LPF resin.[19–21] However, compared with phenol, the steric hindrance in the lignin molecule results in its reaction sites being covered,[22,23] which eventually restricts the application of lignin in the preparation of the PF resin.

Scholars from all over the world have presented various methods to improve the reactivity of lignin, among which phenolation, hydroxymethylation, and demethylation are the three main reactions studied. For example, Podschun *et al.*[24] studied the phenolation process of beech lignin by loading phenol into the substrate at 110 °C with NaOH as the catalyst and found that the maximum phenolation level of each lignin C_9 unit in beech lignin can reach 1.8 phenol; therefore, the reaction sites of lignin to formaldehyde increased. Taverna *et al.*[25] introduced hydroxymethyl groups in black liquor lignin by reacting with formaldehyde in a hot, weakly basic medium for 1 h; the hydroxymethyl lignin obtained was then used to substitute phenol for the preparation of a phenolic resin and it was found that when the substitution ratio of lignin to phenol was 20%, the prepared LPF resin can be used for producing a high pressure laminate. Li *et al.*[26] used S, NaHS, Na_2SO_3, and

Key Laboratory for Green Processing of Chemical Engineering of Xinjiang Bingtuan, School of Chemistry and Chemical Engineering, Shihezi University, Beisi Road, Shihezi, 800032 Xinjiang, China. E-mail: jndxzzl@163.com; zhoun@shzu.edu.cn; Fax: +86-993-2057270; Tel: +86 18909931403

n-dodecyl mercaptan as nucleophilic agents to prepare demethylated lignin (DL) under normal pressure and found that when the substitution rate of lignin to phenol was 30%, the bond strength of 30% demethylated lignin phenol formaldehyde (DLPF) resin could reach 0.94 MPa, which met the standard of exterior-grade plywood panels (0.7 MPa). The TG results indicated that the 30% DLPF resin exhibited good thermal resistance with a weight residue of 57.8% at 700 °C. Although the reactivity of lignin can be greatly improved through phenolation and hydroxymethylation, which are the two commonly used modification methods, they still use phenol and formaldehyde as the raw materials, respectively. In the demethylation process, the demethylating agents such as sulfur powder and *n*-dodecyl mercaptan have low water solubility and poor dispersion, and sodium hydrosulfide has a pungent odor, which makes demethylation a non-green process. Furthermore, in many studies, LPF resins exhibited lower reactivity in the curing reaction; thus, a higher temperature would be needed to achieve complete curing.[27–30] In industrial applications, a lower curing temperature means that less energy and lower cost would be required, which would facilitate the mass production of wood adhesives.

In this paper, a novel mild and green strategy for the preparation of a LPF resin was developed. Alkali lignin was first dissolved in ethylene glycol at room temperature and then, the lignin nanoparticles were precipitated under acidic environment. The morphology, porosity, structure, particle size, and surface charge of the nanolignin particles were characterized by transmission electron microscopy (TEM), Brunauer–Emmett–Teller (BET) measurements, Fourier-transform infrared spectroscopy (FT-IR), dynamic light scattering (DLS), and zeta potential. Nanolignin was then used to substitute phenol partially and was reacted with formaldehyde to synthesize a nanolignin phenol formaldehyde (NLPF) resin. The physical properties, bond strength, and formaldehyde emission of NLPF were tested according to GB/T 17657-2013. The thermosetting and thermal stability properties were evaluated by differential scanning calorimetry (DSC) and thermogravimetric analysis (TG).

2. Experimental

2.1 Experimental reagents

Ethylene glycol, formaldehyde, phenol, and urea, *etc.*, used in this experiment were all obtained from local chemical companies. The alkali lignin used was from Adamas and all the experimental reagents were of analytical grade (AR).

2.2 Preparation and characterization of nanolignin and alkali lignin

1.4 g lignin was dissolved in 50 mL ethylene glycol, the insoluble impurities were removed by filtration after 4 h stirring, and then hydrochloric acid (4.00 cm^3, 0.025 mol L^{-1}) was added to the lignin filtrate solution at the rate of 4 drops per min. The solution was dialyzed in a 3 L beaker for three days with water changed three times a day. The lignin nanoparticles were recovered after precipitating in dilute HCl at pH 2, followed by centrifugation and ultrasonic cleaning to achieve neutral pH.

The morphology of nanolignin and alkali lignin was characterized by TEM. The specific surface area and average pore diameter were measured at 200 °C by BET method. The size distribution and zeta potential were characterized by a nanoparticle sized zeta potential analyzer and the structure was analyzed by FT-IR.

2.3 Preparation and characterization of NLPF adhesives

NLPF was prepared by substituting nanolignin (0, 10, 20, 30, 40, 50, and 60% wt) with different amounts of phenol. The molar ratio of phenol (lignin and phenol) to formaldehyde remained constant at 1.0 : 1.8 in all the tests. First, phenol, proportionally substituted nanolignin or alkali lignin, formaldehyde (37% wt), and 8 mol L^{-1} NaOH (10% wt of the mass of the phenolic resin, added as the catalyst) were placed in a 100 mL three-necked flask. A thermostat water bath was used to maintain a uniform temperature around the flask with stirring. The amount of formaldehyde and NaOH was 2/3 rds of the total amount. The flask was gradually heated to 65 °C in 30 min and maintained at this temperature for 10 min; then, the rest of the NaOH solution as well as formaldehyde solution, and urea (4% wt, used as formaldehyde absorbent) were added to the three-necked flask. The temperature was then slowly increased to 85 °C and was kept constant for 4 h. Finally, the system was cooled to room temperature and the prepared resin was stored at 21 °C until performance characterization.

The structure of NLPF and LPF resins were characterized by FT-IR. The properties of the prepared resins, such as, solid contents, viscosity, free formaldehyde, pH, and formaldehyde emission, were determined using Chinese standard methods (GB/T14074-2006). The dry and wet bond strengths were tested according to GB/T 17657-2013. The curing behavior and thermal stability were evaluated by DSC and TG.

3. Results and discussion

3.1 Characterization of nanolignin and alkali lignin

Fig. 1 shows the TEM images of nanolignin and alkali lignin. Alkali lignin particles (Fig. 1a) are irregularly structured, while the nanolignin particles (Fig. 1b) are much smaller than those of alkali lignin. A part of the nanolignin particles agglomerate, indicating that nanolignin was successfully prepared. As can be seen from Table 1, the specific surface area of lignin is 0.5071 $m^2\ g^{-1}$, which is only about one tenth of the specific surface area of nanolignin (5.3765 $m^2\ g^{-1}$). The pore volume of nanolignin is 0.0092 $cm^3\ g^{-1}$, which is 11 times the pore volume of lignin (0.0008 $cm^3\ g^{-1}$). The high specific surface area and porous structure of nanolignin increase the contact between nanolignin and formaldehyde, which result in the enhanced reactivity of nanolignin.

The size of nanolignin particles was analyzed by DLS; the results are shown in Fig. 2 and Table 2. As can be seen from Fig. 2, the majority of particle sizes of the nanolignin concentrate are between 300 and 500 nm. Table 2 describes the particle

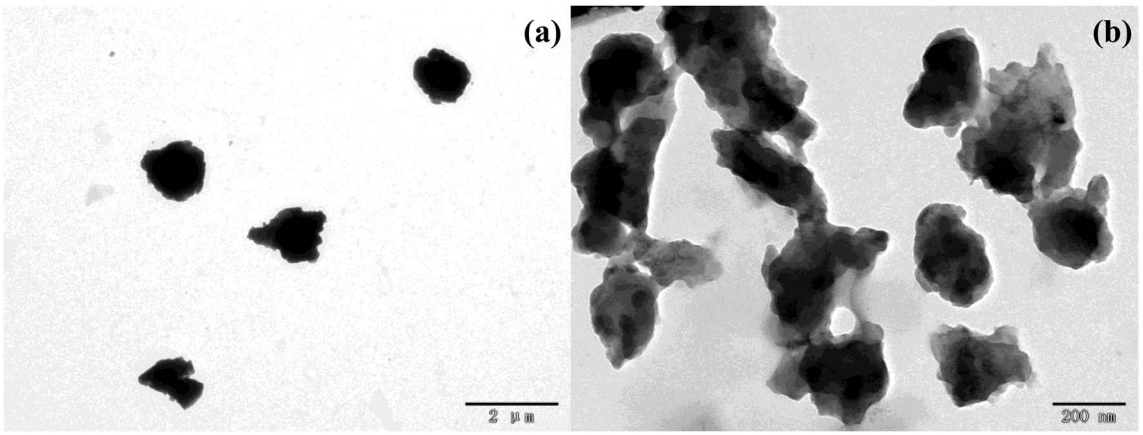

Fig. 1 TEM images of alkali lignin (a) and nanolignin (b).

Table 1 Specific surface area, average pore volume, and pore size of alkali lignin and nanolignin

Sample	Specific surface area ($m^2\ g^{-1}$)	Average pore volume ($cm^3\ g^{-1}$)	Average pore size (nm)
Alkali lignin	0.5071	0.0008	8.51
Nanolignin	5.3765	0.0092	6.91

size distribution from D10 (10% of the total particles are below this diameter) to D90 (90% of the total particles are below this diameter). It can be seen from Table 2 that although the size distribution falls in a wide range, the average size of nanolignin is only 343 nm, with the particle dispersion index (PDI) of nanolignin of 0.327.

Fig. 3 shows the FT-IR spectra absorption peaks of alkali lignin and nanolignin. The characteristic peaks of the main functional groups in the latter were similar to those in the former, indicating the structural similarity between the two kinds of lignin. For example, the absorption band around 3400 cm^{-1} is attributed to the aromatic and aliphatic –OH groups, the absorption band at 2900 cm^{-1} is related to the asymmetric vibration of $-CH_2$, and the stretching vibration of C=C in benzene ring is at 1600 cm^{-1}. However, some differences could still be found, such as the stretching vibration of C=C in benzene ring that changes from 1596 cm^{-1} in alkali

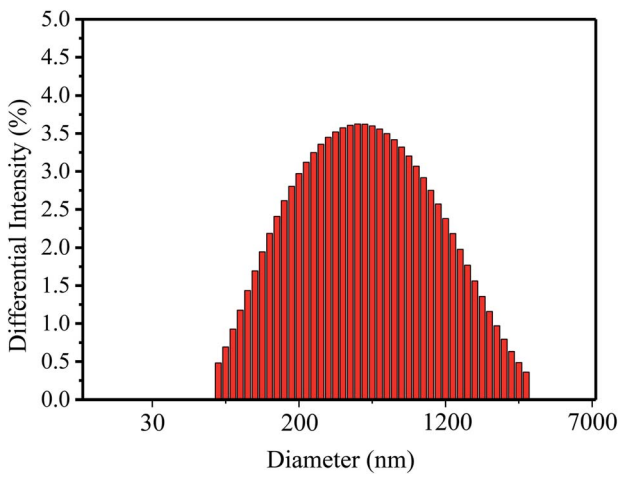

Fig. 2 Particle size distribution of nanolignin.

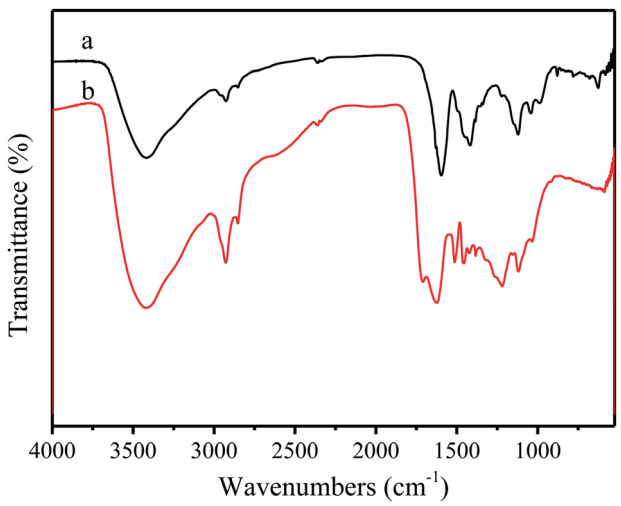

Fig. 3 FT-IR spectra of alkali lignin (a) and nanolignin (b).

Table 2 Particle size distribution of nanolignin

Cumulative Intensity (%)	10	20	30	40	50	60	70	80	90	Average	PDI
Diameter (nm)	134.9	188.9	247.1	323.3	415.8	553.4	723.9	947.1	1358	343.0	0.327

lignin to 1620 cm^{-1} in nanolignin; the stretching vibration peak of ether C–O–C shifted from 1121 cm^{-1} to 1219 cm^{-1}; and the peak of C–O moved from 1041 cm^{-1} to 1119 cm^{-1}. Gupta *et al.*[31] presented that during the preparation of nanolignin, the free –OH in the solution would be bound to the surface of the nanolignin monomer, which causes the absorption peak in the infrared spectrum of nanolignin to move towards longer wavelength.

The surface charge of alkali lignin and nanolignin are characterized by zeta potential at pH 7 (Fig. 4 and Table 3). Nanolignin has a zeta potential of −49.5 mv, which is lower than that of alkali lignin (−17.8 mV), indicating that nanolignin can be easily combined with partially positively charged C atom in the C=O group of formaldehyde.

Since nanolignin has the characteristics of porosity, higher specific surface area, smaller particle size,[32] and lower surface charge, the reaction between formaldehyde and the phenolic units of nanolignin will be more advantageous than that with alkali lignin. Also, it is reported that the introduction of –OH group (FT-IR) could increase the activity of the reaction between nanolignin and formaldehyde, which therefore improves the replacement rate of phenol in nanolignin and reduces the demand for phenol in the synthesis of the NLPF resin.[33]

3.2 Structure and performance analysis of the NLPF resin

The FT-IR spectra of PF, 40% LPF, and 40% NLPF resins are shown in Fig. 5; it was found that the addition of alkali lignin or nanolignin had no significant effect on the PF resin in terms of the chemical structure.

Table 4 shows the performance of different resin samples. It can be seen from Table 4 that as the substitution rate of the NLPF resin replacement by nanolignin increases, the viscosity and density of the NLPF resins increase accordingly because the molecular weight of nanolignin is larger than that of phenol and thus, the addition of nanolignin increases the molecular weight and the internal frictional resistance of the NLPF resin. The viscosity is correspondingly increased meanwhile, compared with liquid phenol; the addition of solid nanolignin does not change the volume of the reaction system and therefore, the density of the NLPF resin is enhanced. The pH of the NLPF resins gradually increases as the substitution rate of phenol by lignin increases because phenol is acidic and the replacement of phenol with neutral nanolignin increases the alkalinity of the NLPF resin. For the solid content of the NLPF resin and free aldehyde, since the reactivity of nanolignin is not as high as that of phenol, in the process of producing NLPF, the reaction between formaldehyde and nanolignin/phenol might be partially completed and some unreacted formaldehyde could lead to decrease and increase in the solid content and free aldehyde of NLPF, respectively, as the substitution rate of phenol replacement with lignin increases. However, the solid content of all the NLPF samples is higher than 40% and the free aldehyde of these NLPF resins (nanolignin replacement ratio ≤ 40%) is lower than 0.3%, which are in accordance with the Chinese standard (GB/T14074-2006). Furthermore, compared with the general 40% LPF resin, the free aldehyde content of the 40% NLPF resin (0.2802%) is less than 1/10th of the free aldehyde content of 40% LPF (3.2007%). The content of free aldehyde in 50% NLPF and 60% NLPF resins is higher than the national standard, indicating that some further work should be conducted to reduce free aldehyde in the NLPF resins.

Compared with other kinds of phenol substituted PF (Table 5), for NLPF, the raw material nanolignin could be prepared at room temperature, while for DLPF, LPBLPF, EHLPF, and PSF, high temperature or high-pressure conditions are required. Furthermore, the bond strength of NLPF is greater than other kinds of phenol substituted PF resins at the same or higher

Table 3 Zeta potential distribution of alkali lignin (a) and nanolignin

Sample	Zeta potential (mV)	Peak 1 (mV)	Peak 2 (mV)
Alkali lignin	−17.8	−20.6	−1.26
Nanolignin	−49.5	−53.7	−39.9

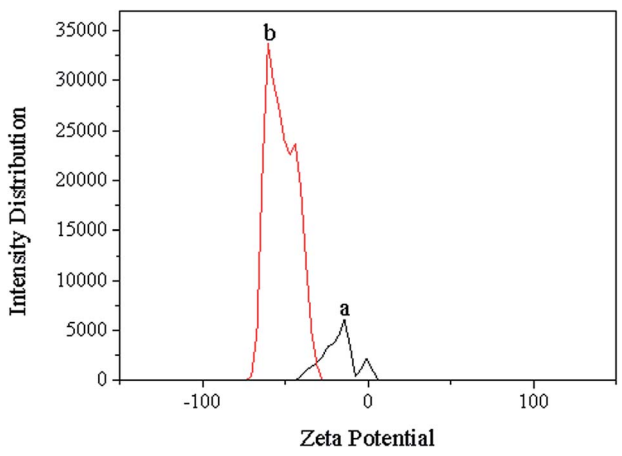

Fig. 4 Zeta potential distribution of alkali lignin (a) and nanolignin (b) at pH 7.

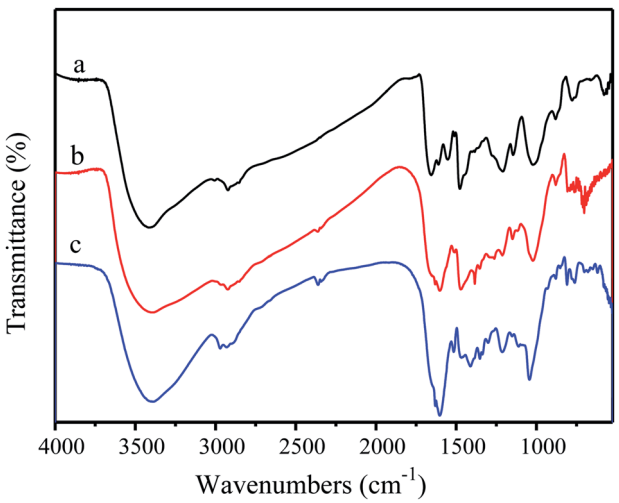

Fig. 5 FT-IR spectra of PF (a), 40% NLPF (b), and 40% LPF (c) resins.

Table 4 Characterization of PF, NLPF, and LPF resins

Sample	Viscosity (mPa S)	pH	Solid contents (%)	Free formaldehyde (wt%)	Density (g cm^{-3})
PF	109	12.63	53.21	0.0009	1.15
10% NLPF	149	12.39	51.51	0.0085	1.13
20% NLPF	184	12.53	49.64	0.0287	1.12
30% NLPF	254	12.72	47.83	0.1167	1.16
40% NLPF	387	13.32	46.90	0.2802	1.18
40% LPF	254	12.50	37.36	3.2007	1.11
50% NLPF	438	13.53	45.63	0.5274	1.19
60% NLPF	512	13.60	44.85	1.0292	1.21
Chinese standard	>60	>7	>35	<0.3	—

substitution rates. The mild preparation conditions of nanolignin and excellent performance of NLPF at high substitution rate could reduce the energy and production costs, and promote the application of the renewable material nanolignin instead of fossil material phenol in the industrial production of NLPF resins.

Fig. 6 shows the tensile strength of PF, NLPF, and LPF. Table 6 gives the corresponding maximum failure load. According to the Chinese national standard GB/T 17657-2013, the bond strength of plywood is calculated as follows:

$$P = \frac{F_{\max}}{b \times l} \quad (1)$$

where P (MPa) is the bond strength of the plywood, $F_{\max}$ (N) is the maximum failure load of the plywood, and b and l are the width and the length of the shear section of the plywood.

Fig. 7 describes the bond strength of different resin samples and the formaldehyde emission from plywoods prepared with these resins. The formaldehyde emission of PF and all the substituted NLPF samples are lower than that of the Chinese standard (E_0), which means that the plywood prepared by NLPF can be applied to various indoor and outdoor environments. In addition, it can be seen that the dry and wet bond strengths of the NLPF adhesives show a tendency to rise first and then fall. The bond strength of all the NLPF adhesives is higher than that of the PF resin, except that of 60% NLPF. The bond strength of NLPF keeps increasing as the substitution rate of phenol with nanolignin increases from 10% to 30%. When the substitution rate of phenol with nanolignin is 30%, the dry and wet bond strengths of the plywood reach 1.59 MPa and 0.89 MPa, respectively; as the substitution rate increases to 40%, the dry and wet bond strengths reduce to 1.30 MPa and 0.85 MPa, which nevertheless increase by 14.6% and 5.3% in comparison to those for 40% LPF, respectively. The addition of nanolignin increases the dry and wet bond strengths of the NLPF adhesive[36] because nanolignin is an excellent cross-linking agent for the synthesis of NLPF resins compared with phenol. However, since nanolignin is less reactive than phenol, excess nanolignin (lignin to phenol ratio: 40% to 60%) would make the synthesis of the NLPF resin incomplete and the bond strength decrease, which however, is still higher than the national standard (0.7 MPa). For industrial production, the higher substitution rate of

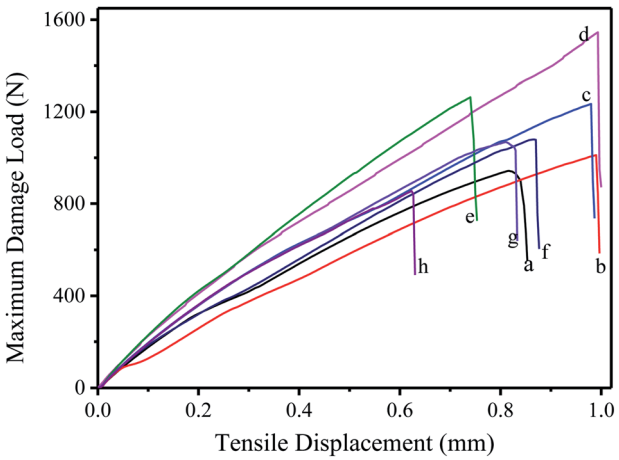

Fig. 6 The tensile strength curve of PF, NLPF, and LPF resins. (a) PF, (b) 10% NLPF, (c) 20% NLPF, (d) 30% NLPF, (e) 40% NLPF, (f) 40% LPF, (g) 50% NLPF, (h) 60% NLPF.

Table 5 Comparison of different kinds of phenol substituted PF resins

Resin type	Substitutes for phenol	Substitution condition	Substitution rate (%)	Free formaldehyde (%)	Dry bond strength (MPa)
DLPF[12]	Degraded liquids (DL)	260 °C 3.4 MPa	40	0.13	1.04
LPBLPF[34]	Liquefaction product of bagasse lignin (LPBL)	Microwave 200 °C	20	—	1.02
EHLPF[14]	Enzymatic hydrolysis lignin (EHL)	65 °C	20	0.24	1.15
PSF[35]	Soya (S)	85 °C	40	—	—
NLPF	Nanolignin (NL)	Room temperature	40	0.28	1.30

Table 6 Maximum damage load of PF, NLPF, and LPF resins

Sample	PF	10% NLPF	20% NLPF	30% NLPF	40% NLPF	40% LPF	50% NLPF	60% NLPF
Maximum damage load (N)	943.04	1011.66	1234.34	1545.06	1263.74	1079.44	1069.40	855.40

phenol with nanolignin means that less phenol will be used in the synthesis of NLPF, which would facilitate the green production of wood adhesives and exert a profound and significant effect on the conservation of fossil resources.

In the process of measuring the bond strength of the plywood, when the bond strength is greater than the strength of the wood, the wood is first broken by the external force and the bond layer remains stable, and then the wood failure rate of the plywood reaches 100%. When the bond strength is similar to or less than the strength of the wood, both the wood and the bond layer are broken to some extent and then, the wood failure rate of the plywood reduces correspondingly. The wood failure percentage of PF, NLPF, and LPF resins is shown in Table 7. The wood damage rate of most of the plywoods is 100%, which means that the bond strength of NLPF resins is higher than the strength of pine wood, even for 10% NLPF whose wet bond strength is 0.62 MPa. For the wet bond strength of 40% LPF and 60% NLPF, 80% and 60% wood failure are obtained because the free formaldehyde of 40% LPF and 60% NLPF resins are high; thus, the water resistance of the two resins decreases and the wet bond strength is also reduced.

3.3 Curing behavior analysis of NLPF resins

Fig. 8 shows the DSC diagram of PF, 40% LPF, and 40% NLPF resins. It can be seen that the exothermic peaks produced in the process of the curing reaction varied from 180.3 °C (PF resin) to 145.4 °C (40% NLPF) and 186.1 °C (40% LPF). Compared with PF and 40% LPF resin, the peak temperature of the 40% NLPF resin decreases significantly, and a wider exothermic peak is obtained, indicating that NLPF has better reactivity than PF and LPF resins in the curing reaction and that the curing reaction can occur in a wider temperature range. It is reported that the smaller size of nanolignin causes the –OH functional groups, which are surrounded by highly crosslinked three-dimensional network in the lignin structure, to be more exposed on the nanolignin monomer, which makes nanolignin a remarkable crosslinking agent in the curing reaction.[37,38] The 40% LPF resin gives a sharp exothermic peak and a higher peak temperature than the ordinary PF resin, which might be because the high content of free formaldehyde in LPF triggers the crosslinking reaction in the curing process. Meanwhile, compared with nanolignin, the lower reactivity of alkali lignin leads to a higher curing temperature for LPF than that for NLPF.[39] It is well known that a lower curing temperature of the resins will bring about reduced temperature at hot pressing and reduction in cost for producing artificial wood boards. The excellent curing performance makes economic sense for NLPF to be widely used in wood-based panel manufacturing.

The thermal decomposition and thermal stability of the PF, NLPF, and LPF resins were measured and the results are shown in Fig. 9. The thermal degradation of the resins is mainly divided into three parts: post-curing (100–250 °C), thermal

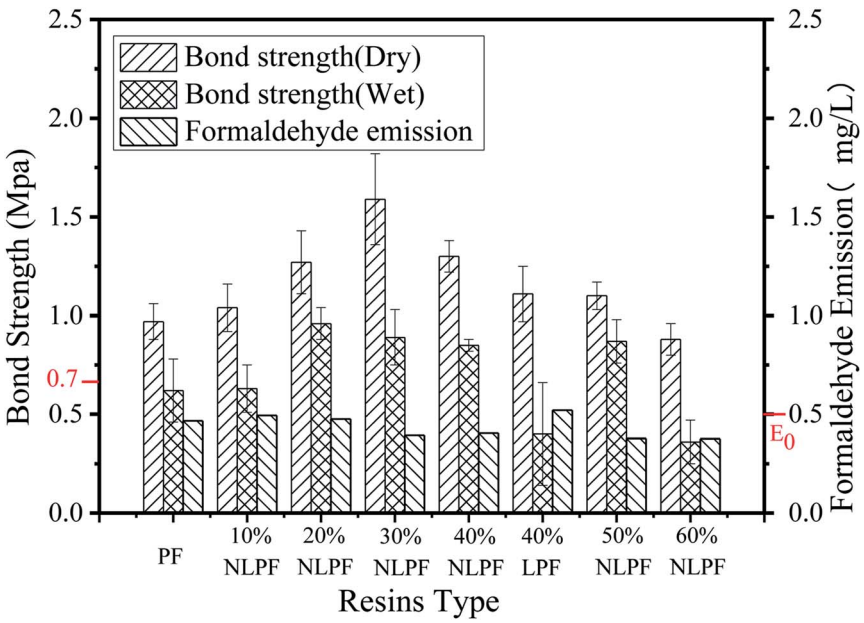

Fig. 7 Bond strength and formaldehyde emission from plywood bonded with PF, LPF, and NLPF resins.

Table 7 Characterization of plywoods bonded with PF, NLPF, and LPF resins

Sample	Dry bond strength (MPa)	Wood failure percentage (%)	Wet bond strength (MPa)	Wood failure percentage (%)	Formaldehyde emission (mg L^{-1})
PF	0.97 (0.09)	100	0.62 (0.16)	100	0.4669
10% NLPF	1.04 (0.12)	100	0.63 (0.12)	100	0.4937
20% NLPF	1.27 (0.16)	100	0.96 (0.08)	100	0.4758
30% NLPF	1.59 (0.23)	100	0.89 (0.14)	100	0.3929
40% NLPF	1.30 (0.08)	100	0.85 (0.02)	100	0.4043
40% LPF	1.11 (0.14)	100	0.40 (0.56)	80	0.5205
50% NLPF	1.10 (0.07)	100	0.87 (0.11)	100	0.3778
60% NLPF	0.88 (0.08)	100	0.36 (0.11)	60	0.3758
Chinese standard	>0.7	—	>0.7	—	<0.5 (E_0)

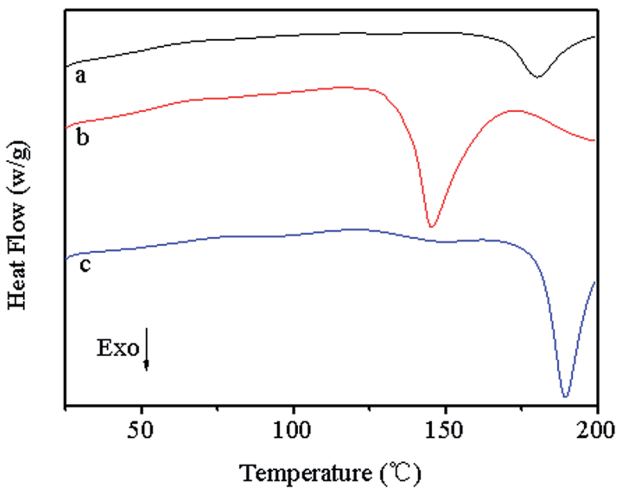

Fig. 8 DSC diagram of PF (a), 40% NLPF (b), and 40% LPF (c) resins.

reforming (250–500 °C), and ring-stripping (500–800 °C). In the post-curing part, the heat loss is generated by the escape of water produced in the condensation reaction of the methylol groups. It can be seen that when the temperature reaches 250 °C, the residual ratio of the PF resin is 87%, the residual ratio of the 40% NLPF resin is 82%, and the residual ratio of the 40% LPF resin is 75%. In the process of thermal reforming, the heat loss is caused by water formed in the condensation reaction between the methylene group and the phenolic hydroxyl group. The residual ratio of PF, 40% NLPF, and 40% LPF resins comes to 68%, 55%, and 48%, respectively, when the temperature reaches 500 °C. In the ring-stripping part, the heat loss is caused by carbon monoxide and methane formed in the degradation of the methylene bridge. It can be seen from the figure that when the temperature reaches 800 °C, the residual ratio of PF, 40% NLPF, and 40% LPF resins is 54%, 45%, and 40%, respectively. Because nanolignin is not as reactive as phenol, 40% NLPF has a lower solid residue rate than PF. However, compared with the 40% LPF resin, the 40% NLPF resin exhibits a larger residual weight at 800 °C, which demonstrates the better reactivity of nanolignin than alkali lignin. The introduction of more reactive nanolignin could facilitate higher degree of polymerization of the phenolic resins, thereby resulting in more weight residues at high temperature.

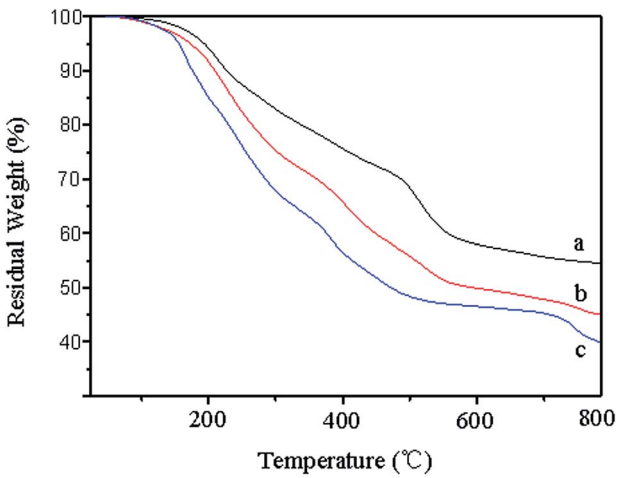

Fig. 9 TG curve of PF (a), 40% NLPF (b), and 40% LPF (c) resins.

4. Conclusions

Nanolignin with a high specific surface area, porous structure, and lower zeta potential with an average particle size of about 300 nm was prepared, used as the raw material to substitute phenol partially, and to combine with formaldehyde to produce wood adhesives. The NLPF with phenol substitution with nanolignin degree of 40% had a bond strength of 1.30 ± 0.08 MPa, which was 1.85 times of the national grade 1 plywood standard (0.7 MPa). The formaldehyde emission amount of the plywood prepared from 40% NLPF was 0.40 mg L^{-1}, which was E_0 grade and met the GB/T 14732-2006 standard. The curing behavior analysis showed that the substitution of phenol with nanolignin significantly reduced the curing temperature from 186.2 °C (40% LPF) to 145.4 °C (40% NLPF). The thermal stability result indicated that the residual rate increased from 40% (40% LPF) to 45% (40% NLPF) at 800 °C. Compared with the conventional technology, the reaction conditions were mild, phenol and formaldehyde were not used, and no other by-products were produced in the process of modification. The present study provides a new idea for the green production of phenolic resins.

Conflicts of interest

There are no conflicts to declare.

Acknowledgements

We gratefully acknowledge the financial support provided by National Natural Science Foundation of China (Grant No. 21464011).

References

1 M. Thébault, A. Kandelbauer, E. Z. Rusch, R. Putz, S. Jury and I. Eicher, *Eur. Polym. J.*, 2018, **104**, 90–98.
2 J. Li, J. Zhang, S. Zhang, Q. Gao, J. Li and W. Zhang, *Polymers*, 2017, **9**(9), 428–445.
3 Y. Guo, L. Hu, P. Jia, B. Zhang and Y. Zhou, *Korean J. Chem. Eng.*, 2018, **35**(1), 298–302.
4 R. Zhang, X. Jin, X. Wen, Q. Chen and D. Qin, *Int. J. Adhes. Adhes.*, 2018, **81**, 79–82.
5 I. Kalami, M. Arefmanesh, E. Master and M. Nejad, *J. Appl. Polym. Sci.*, 2017, **134**(30), 45124.
6 L. Klapiszewski, A. Jamrozik, B. Strzemiecka, D. Matykiewicz, A. Voelkel and T. Jesionowski, *Int. J. Mol. Sci.*, 2017, **18**(6), 1224–1243.
7 W. Qiao, S. Li, G. Guo, S. Han, S. Ren and Y. Ma, *J. Ind. Eng. Chem.*, 2015, **21**, 1417–1422.
8 R. J. Li, J. Gutierrez, Y. . L. Chung, C. Frank, S. Billington and E. S. Sattely, *Green Chem.*, 2018, **20**(7), 1459–1466.
9 J. Park, H. Hwang, J. Y. Kim and J. W. Choi, *Environ. Technol.*, 2018, 201–207.
10 W. Zhang, Y. Ma, C. Wang, S. Li, M. Zhang and F. Chu, *Ind. Crops Prod.*, 2013, **43**(1), 326–333.
11 Z. Li, Z. Cai, Q. Zeng, T. Zhang, L. J. France, C. Song, Y. Zhang, H. He, L. Jiang, J. Long and X. Li, *Green Chem.*, 2018, **20**(16), 3743–3752.
12 L. Yan, Y. Cui, G. Gou, Q. Wang, M. Jiang, S. Zhang, D. Hui, J. Gou and Z. Zhou, *Composites, Part B*, 2017, **112**, 8–14.
13 Y. Hamed and P. Antonio, *J. Adhes.*, 2018, **94**(2), 143–154.
14 Y. Jin, X. Cheng and Z. Zheng, *Bioresour. Technol.*, 2010, **101**(6), 2046–2048.
15 S. Yang, Y. Zhang and T. Yuan, *J. Appl. Polym. Sci.*, 2015, **132**(36), 42493.
16 Z. Shuai, L. Tuan and H. Cheng, *Green Chem.*, 2018, **20**(13), 2995–3000.
17 Y. Zhang, J. Wu and H. Li, *ACS Sustainable Chem. Eng.*, 2017, **5**(8), 7269–7277.
18 P. Cavalcante, G. Francisca, S. Lima, *et al.*, *Ind. Crops Prod.*, 2017, **96**, 80–90.
19 M. Zhao, J. Jing and Y. Zhu, *Int. J. Adhes. Adhes.*, 2016, **64**, 163–167.
20 W. Qiao, S. Li and F. Xu, *Polym. Polym. Compos.*, 2016, **24**(2), 99–106.
21 M. Hussin, H. Zhang and N. Aziz, *Beni-Suef University Journal of Basic and Applied Sciences*, 2017, **6**(4), 409–418.
22 M. Ghorbani, F. Liebner and H. V. Herwijnen, *Eur. J. Wood Wood Prod.*, 2018, **76**(1), 251–258.
23 G. Masoumeh, J. Konnerth and H. V. Herwijnen, *J. Appl. Polym. Sci.*, 2018, **135**(8), 45893.
24 J. Podschun, B. Saake and R. Lehnen, *Eur. Polym. J.*, 2015, **67**, 1–11.
25 M. E. Taverna, O. Tassara and J. Moran, *Waste Biomass Valorization*, 2019, **10**(3), 585–597.
26 J. Li, W. Wang and S. Zhang, *RSC Adv.*, 2016, **6**(71), 67435–67443.
27 Y. Jin, X. C. Li and F. Z. Xiao, *J. Mater. Sci.*, 2018, **53**(20), 14185–14203.
28 P. Deng, Y. Shi and Y. Liu, *Appl. Surf. Sci.*, 2018, **427**, 894–904.
29 H. R. Taghiyari, H. Rangavar and O. F. Bibalan, *BioResources*, 2011, **6**(4), 4067–4075.
30 A. Kumar, A. Gupta and K. V. Sharma, *Eur. J. Wood Wood Prod.*, 2013, **71**(2), 193–198.
31 A. Gupta, M. Smita and S. Nayak, *Mater. Focus*, 2014, **3**(6), 444–454.
32 W. Yang, M. Rallini and M. Natali, *Mater. Des.*, 2019, **161**, 55–63.
33 S. Yang, J. Wu and Y. Zhang, *J. Biobased Mater. Bioenergy*, 2015, **9**(2), 266–272.
34 Y. Li, B. Li and F. Du, *J. Appl. Polym. Sci.*, 2017, **134**(10), 44510.
35 B. S. Mamatha, D. Sujatha and S. K. Nath, *J. Indian Acad. Wood Sci.*, 2011, **8**(2), 112–115.
36 M. Wang, M. Leitch and C. Xu, *Eur. Polym. J.*, 2009, **45**(12), 3380–3388.
37 S. Kalami, N. Chen and H. Borazjani, *Ind. Crops Prod.*, 2018, **125**, 520–528.
38 S. Nair, S. Sharma and Y. Pu, *ChemSusChem*, 2014, **7**(12), 3513–3520.
39 W. Lee, K. Chang and I. Tseng, *J. Appl. Polym. Sci.*, 2012, **124**(6), 4782–4788.

